International Journal of Current Research and Techniques (IJCRT)
E-ISSN: 2349-3194 (Online) | P-ISSN: 2348-4446 (Print)
UGC Approved Journal No: 47722 [No: 2616]
DOI: https://doi.org/10.5281/ZENODO.15273418

A Meander Line Patch MIMO Antenna for Synthetic Aperture Radar Application

M. Anukeerthana, *PG Scholar, Department of Electronics and Communication Engineering, Government College of Engineering, Salem, Tamil Nadu, India*

Dr. G. Kavithaa, *Associate Professor, Department of Electronics and Communication Engineering, Government College of Engineering, Salem, Tamil Nadu, India*

Manuscript Received: Apr 09, 2025; Revised: Apr 24, 2025; Published: Apr 24, 2025

Abstract: The research presents the design of a meander line patch MIMO antenna for synthetic aperture radar applications, which resonates at 1.3 GHz on L-band and 3.05 and 3.8170 GHz on S-band frequencies. The MIMO antenna is built on a FR4 substrate with a dielectric constant of 4.4 and a thickness of 1.6 mm, and it is designed using the ANSYS HFSS software program. This design focuses on optimizing radiation patterns while remaining compact and simple to fabricate. The proposed antenna has a return loss of below -20 dB, VSWR < 1.5, an axial ratio of < 3dB. The simulation results illustrate how well the MIMO antenna effectively performs for SAR applications, such as vegetation monitoring, soil moisture, GPS, and disaster management.

Keywords: Frequency Structure Simulator (ANSYS HFSS), Voltage Standing Wave Ratio (VSWR), Gigahertz (GHz), Return Loss (RL), Flame Retardant for Woven Glass Reinforced Epoxy Resin (FR4)

1. Introduction:

Synthetic Aperture Radar (SAR) has emerged as a powerful remote sensing technology widely utilized in applications such as vegetation monitoring, soil moisture estimation, disaster management, and GPS-based navigation. Microstrip patch antennas are commonly used in SAR applications due to their lightweight, low-profile, and easy fabrication features. However, conventional patch antennas often face challenges in achieving wideband performance, high gain, and minimal mutual coupling, particularly in multi- input multi-output (MIMO) configurations. In this research, a meander line patch MIMO antenna is designed and simulated for SAR applications. The proposed antenna operates at L-band (1.3 GHz) and S- band (3.05 GHz and 3.817 GHz) frequencies, making it suitable for remote sensing applications. Built on an FR4 substrate with a dielectric constant of 4.4 and a thickness of 1.6 mm, the antenna is designed using ANSYS HFSS software to achieve optimized performance. The design focuses on ensuring low return loss, voltage standing wave ratio (VSWR) below 1.5, low mutual coupling, and an axial ratio below 3 dB to support circular polarization.

2. Related Works

S. C, N. D. M, and J. M. [1] this work achieved dual-band operation by utilizing an annular ring structure with optimized feed mechanisms to ensure circular polarization. Y. Cheng and Y. Dong [2] presented a wideband circularly polarized split patch antenna loaded with suspended rods, which enhanced bandwidth and circular polarization performance. M. Sun, Z. Zhang, F. Zhang and A. Chen [3] introduced an L/S multiband frequency-reconfigurable antenna designed for satellite applications. The design incorporated tunable elements to achieve frequency reconfiguration across multiple bands. N. Rasool, H. Kama, M. Abdul Basit and M. Abdullah [4] developed a low-profile, high-gain, ultra-lightweight circularly polarized annular ring slot antenna for airborne and airship applications. M. M. Bilgic and K. Yegin [5] designed a modified annular ring antenna tailored for GPS and Satellite Digital Audio Radio Service (SDARS) applications in automotive systems.

3. Objective

The primary objective of this project is to design and simulate a meander line patch Multiple-Input Multiple-Output (MIMO) antenna that operates at L-band (1.3 GHz) and S-band (3.0 GHz and 3.81 GHz) frequencies for Synthetic Aperture Radar (SAR) applications. A key goal is to achieve a return loss below -20 dB and VSWR <2 to ensure excellent impedance matching across the target frequencies while incorporating circular polarization with an axial ratio to enhance polarization purity and signal reception.

4. Design Software

ANSYS HFSS is a 3D electromagnetic (EM) simulation software for designing and simulating high-frequency electronic products. ANSYS HFSS (High- Frequency Structure Simulator) is a comprehensive simulation tool widely used for designing and analyzing high- frequency electromagnetic structures in industries such as telecommunications, aerospace, defense, and electronics.

5. Proposed Design Methodology

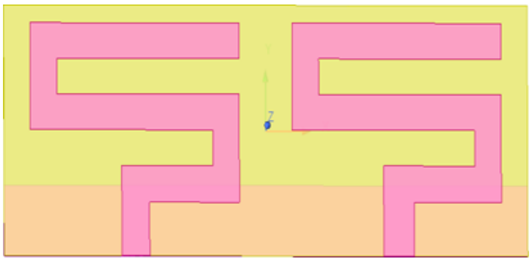

Figure-1 Meander line patch MIMO antenna

The proposed meander line patch MIMO antenna is designed to operate at L-band (1.3 GHz) and S-band (3.05 GHz and 3.817 GHz), making it well-suited for Synthetic Aperture Radar (SAR) applications. The shape and structure of the antenna play a crucial role in achieving multi-band operation, and performance.

Meander Line Patch Structure

The meander line configuration increases the electrical path length, allowing resonance at lower frequencies without increasing the overall antenna size. The L-band resonance at 1.3 GHz is critical for deep penetration in applications like vegetation monitoring and soil moisture estimation. The S-band resonances at 3.05 GHz and 3.817 GHz provide improved resolution and data acquisition. The multi-band operation is achieved by precisely tuning the patch dimensions and meander line structure.

Edge Feeding Technique

The antenna employs an edge feeding technique, which is a type of microstrip feed that provides a direct connection to the patch. Edge feeding is a simple and effective feeding technique that allows for easy fabrication and integration into SAR platforms.

Design Equation of Rectangular Microstrip Patch Antenna

F_0=1.3,3.05,3.8170GHz, C=3x 10^8m/s

Width of the patch,

$$W = \frac{c}{2f\sqrt{\frac{\varepsilon_\gamma+1}{2}}} \quad (1)$$

Length of the patch,

$$L = \frac{c}{2f\sqrt{\varepsilon_{eff}}} - 2(\Delta L) \quad (2)$$

Width of the Substrate,

$$W_s = 6\,h + w \quad (3)$$

Length of the Substrate

$$L_S = 6\,h + L \quad (4)$$

Length of the Ground

$$L_g = L+6h \quad (5)$$

Width of the Ground

$$W_g = w+6\,h \quad (6)$$

Where,
c is the velocity of light
f_0 is resonant frequency,
εr is the relative permittivity
sreff is the effective relative permittivity,
h height of substrate
W is the width of the substrate.

Design Measurements of Proposed Antenna

From the equation [1], W_p=75.5 mm
From the equation [2], L_p=50.31 mm
From the equation [3], W_s=88.76 mm
From the equation [4], Ls=70.31 mm
From the equation [5], W_g=217.12 mm
From the equation [6], L_g=19.9 mm

Table-1 Dimensions of Proposed Antenna

Name of the parameters	**Length (mm)**
Length of the Substrate (Ls)	70.31
Width of the Substrate (W_s)	88.76
Length of the Patch (L_p)	75.5
Width of the Patch (W_p)	50.31
Relative permittivity of the substrate (FR4), εr	4.4
Height of the Substrate (H_s)	1.6
Length of the Feedline (L_f)	15
Width of the Feedline (W_f)	10.7
Width of the Ground (W_g)	217.12
Length of the Ground (L_g)	19.9

Proposed Antenna Design

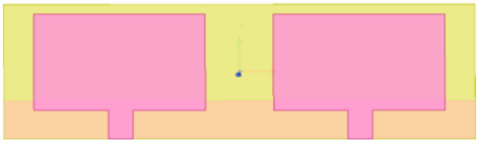

Figure-2 First stage of MIMO antenna

The first stage of MIMO antenna with simple patch and defective ground under the substrate

International Journal of Current Research and Techniques (IJCRT)
E-ISSN: 2349-3194 (Online) | P-ISSN: 2348-4446 (Print)
UGC Approved Journal No: 47722 [No: 2616]
DOI: https://doi.org/10.5281/ZENODO.15273418

Figure-3 Second stage of antenna with slot

The second stage of MIMO antenna with single rectangular slot on patch.

Figure-4 Third stage of MIMO antenna

The third stage of MIMO antenna with double rectangular slot on patch

Figure-5 final stage of meander line antenna

The final proposed design of a meander line patch MIMO antenna at operating at dual band in the frequencies of 1.3 GHz (L-band) and 3.05 and 3.8170 GHz (S- band), the patch having a length of 50.31 mm and the width of 75.5 mm with εr of4.4 the height of 1.6mm.

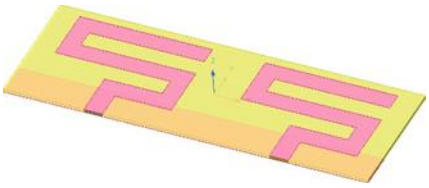

Figure-6 3D View of MIMO antenna design

6. Results in HFSS Software

On the Project Manager result, do a right-click. Choose to Create a Data Report for Modal Solutions. Decide on a rectangular plot. After choosing the S parameter, click S (1,1), then dB. Select "New Report." It displays a return loss plot. Plots are generated in the same spirit for VSWR, gain, directivity, and radiation pattern.

Return Loss On Various Stages

Figure-7 RL at port 1 on various stages

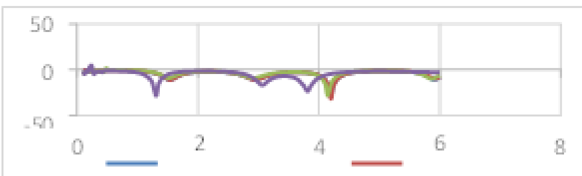

International Journal of Current Research and Techniques (IJCRT)
E-ISSN: 2349-3194 (Online) | P-ISSN: 2348-4446 (Print)
UGC Approved Journal No: 47722 [No: 2616]
DOI: https://doi.org/10.5281/ZENODO.15273418

Figure-8 RL at port 2 on various stages

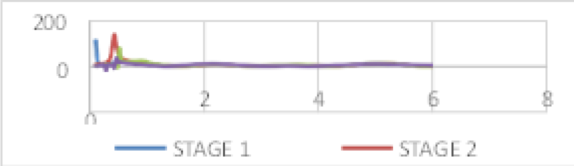

Figure-9 VSWR at port 1 on various stages

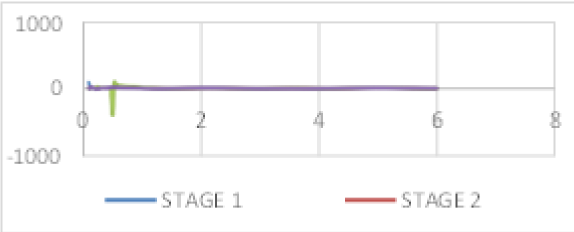

Figure-10 VSWR at port 2 on various stages

Table 2: Comparison of Return Loss And VSWR On Various Stages

Stages		Freq (GHz)	Return loss(dB)	VSWR
First	Port 1	1.3	-3.9929	4.4
		3.05	-9.5768	1.9
		3.8170	-3.4381	5.1185
	Port 2	1.3	-4.1125	4.3028
		3.05	-8.7315	2.1543
		3.8170	-3.3584	5.2369
Second	Port 1	1.3	-4.2139	4.2030
		3.05	-9.5021	2.0070
		3.8170	-3.2583	5.3939
	Port 2	1.3	-4.0824	4.3334
		3.05	-9.5013	2.0071
		3.8170	-3.3929	5.1850
Third	Port 1	1.3	-3.4822	5.0554
		3.05	-7.1601	2.5625
		3.8170	-3.1465	5.5813
	Port 2	1.3	-3.6168	4.8723
		3.05	-7.1459	2.5666
		3.8170	-3.3148	5.3041
FINAL	Port 1	1.3	-31.2656	1.0562
		3.05	-14.6844	1.4522
		3.8170	-22.0701	1.1711
	Port 2	1.3	-27.8839	1.0841
		3.05	-16.6197	1.3463

		3.8170	-23.4399	1.1443

7. Results

Return loss

Lower return loss indicates better impedance matching, meaning more power is being transmitted and less is being reflected. This antenna achieved return loss of - 31.2656 dB, -14.6844 dB, -22.0701 dB on 1.3 GHz, 3.05 and 3.8170 GHz at port 1.

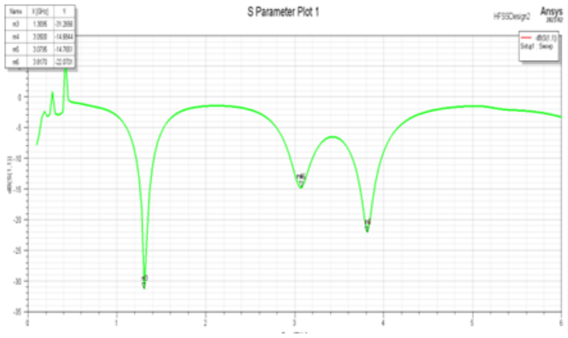

Figure-11 Return loss at port 1

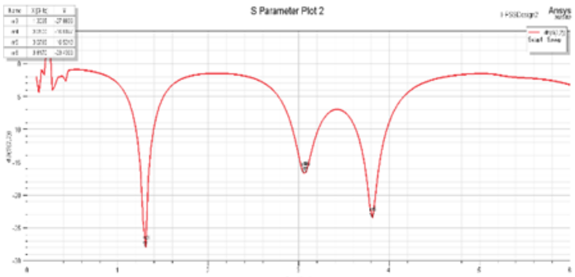

Figure-12 Return loss at port 2

This antenna achieved return loss of - 27.8839 dB, -16.6197 dB, -23.4399 dB on 1.3 GHz, 3.05 and 3.8170 GHz at port 2.

VSWR

VSWR is the ratio of the maximum voltage to the minimum voltage in a standing wave pattern along a transmission line. This antenna achieved VSWR of 1.0562, 1.4522, 1.1711 on 1.3 GHz, 3.05 GHz and 3.8170 GHz at port 1.

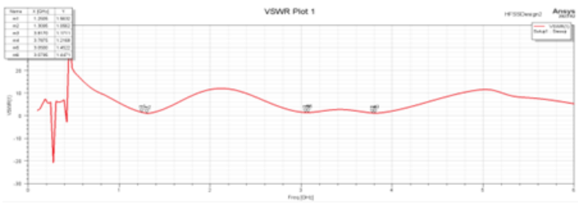

Figure-13 VSWR at port 1

International Journal of Current Research and Techniques (IJCRT)
E-ISSN: 2349-3194 (Online) | P-ISSN: 2348-4446 (Print)
UGC Approved Journal No: 47722 [No: 2616]
DOI: https://doi.org/10.5281/ZENODO.15273418

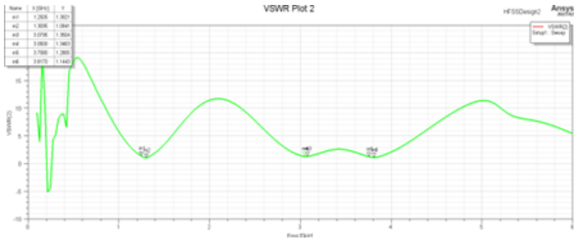

Figure-14 VSWR at port 2

VSWR of 1.0841, 1.3463, 1.1443 on 1.3 GHz, 3.05 GHz and 3.8170 GHz at port 2.

Mutual Coupling

Mutual coupling in antennas refers to the interaction between two or more antenna elements that are located in close proximity to each other. It indicates less interference between two elements of MIMO antenna.

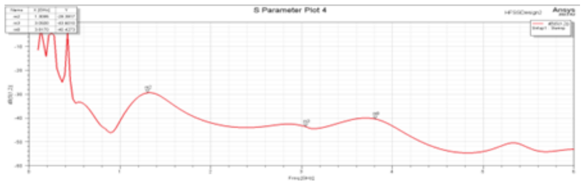

Figure-15 Mutual coupling at port1 and port2

This antenna achieved mutual coupling between port 1 and port 2 is -29.3917, - 43.6010, -40.4278 on 1.3 GHz, 3.05 GHz and 3.8170 GHz

Axial Ratio

The axial ratio (AR) is the ratio between the major and minor axis of a polarized antenna pattern. It is essential to minimize the axial ratio for applications that require circular polarization, such as SAR systems. If it is less than 3 dB then circularly polarized is achieved. This antenna achieved an axial ratio is 2.8919.

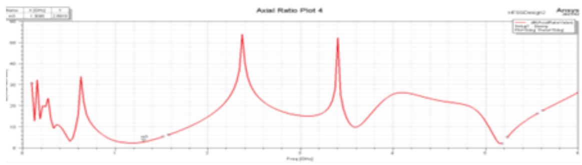

Figure-16 Axial ratio

Co-Polarization and Cross- Polarization

The desired polarization component in the radiated field is Co-Polarization. The undesired polarization orthogonal to the desired one is Cross-Polarization

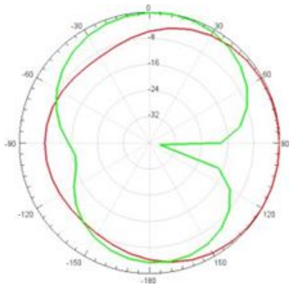

Figure-17 Co-Polarization

International Journal of Current Research and Techniques (IJCRT)
E-ISSN: 2349-3194 (Online) | P-ISSN: 2348-4446 (Print)
UGC Approved Journal No: 47722 [No: 2616]
DOI: https://doi.org/10.5281/ZENODO.15273418

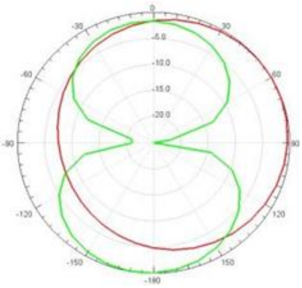

Figure-18 Cross-Polarization

Gain

Gain is a measure of how much power is transmitted in a specific direction compared to an isotropic antenna. Gain is commonly expressed in dBi.

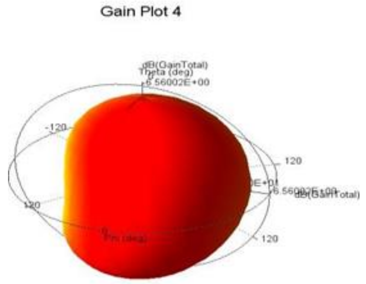

Figure-19 Gain

Table-3 Simulation Results

Results	Frequency	Port 1	Port 2
Return loss(dB)	1.3 GHz	-31.2656	-27.8839
	3.05 GHz	-14.6844	-16.6197
	3.8170 GHz	-22.0701	-23.4399
VSWR	1.3 GHz	1.0562	1.0841
	3.05 GHz	1.4522	1.3463
	3.8170 GHz	1.1711	1.1443
Mutual coupling(dB)	1.3 GHz	-29.3917	-29.3917
	3.05 GHz	-43.6010	-43.6010
	3.8170 GHz	-40.4278	-40.4278

Check for updates

8. Conclusion

The design and simulation of a meander line patch MIMO antenna for Synthetic Aperture Radar (SAR) applications demonstrate its effectiveness for remote sensing. The return loss values of - 31.2656 dB, -14.6844 dB, -22.0701 dB and -27.8839 dB, -16.6197 dB, -23.4399 dB on 1.3 GHz, 3.05 GHz, and 3.817 GHz at port1 and port 2 respectively, ensures minimizing reflected power and ensuring efficient signal transmission. The VSWR values of 1.0562, 1.4471, 1.1711 and 1.0841, 1.3463, 1.1443 on 1.3 GHz, 3.05 GHz, and 3.817 GHz at port1 and port 2 respectively, are close to the ideal, indicating that the antenna is well-matched to the transmission line, resulting in minimal signal loss and high efficiency. The mutual coupling of over 29 dB between two sports ensures low interference, while the axial ratio of 2.8919 dB highlights circular polarization for enhanced signal reception. By utilizing the FR4 substrate, meander line patch, and feed pattern, this design meets the stringent requirements of SAR applications such as vegetation monitoring, soil moisture analysis, disaster management.

7.References

[1] (2022). Dual-Band Circularly Polarized Annular Ring Patch Antenna for GPS-Aided GEO-Augmented Navigation Receivers. IEEE Antennas and Wireless Propagation Letters, 21(9), 1737–1741. https://doi.org/10.1109/LAWP.2022.3178980

[2] Cheng, Y., & Dong, Y. (2021). Wideband Circularly Polarized Split Patch Antenna Loaded With Suspended Rods. IEEE Antennas and Wireless Propagation Letters, 20(2), 229–233. https://doi.org/10.1109/LAWP.2020.3045988

[3] (2019). L/S Multiband Frequency-Reconfigurable Antenna for Satellite Applications. IEEE Antennas and Wireless Propagation Letters, 18(12), 2617–2621. https://doi.org/10.1109/LAWP.2019.2945624

[4] Rasool, N., Kama, H., Abdul Basit, M., & Abdullah, M. (2019). A Low Profile High Gain Ultra Lightweight Circularly Polarized Annular Ring Slot Antenna for Airborne and Airship Applications. IEEE Access, 7, 155048–155056. https://doi.org/10.1109/ACCESS.2019.2949683

[5] Bilgic, M. M., & Yegin, K. (2016). Modified Annular Ring Antenna for GPS and SDARS Automotive Applications. IEEE Antennas and Wireless Propagation Letters, 15, 1442–1445. https://doi.org/10.1109/LAWP.2015.2512558

[6] Li, L., Huang, Y., Zhou, L., & Wang, F. (2016). Triple-Band Antenna With Shorted Annular Ring for High-Precision GNSS Applications. IEEE Antennas and Wireless Propagation Letters, 15, 942–945. https://doi.org/10.1109/LAWP.2015.2482604

[7] Nguyen, M. T., Alhaj Hasan, A. F., & Gazizov, T. R. (2024). Recommendations on Designing Wire Grid Conical Horn Structures for Sparse Antenna Generation. In 2024 International Conference on Actual Problems of Electron Devices Engineering (APEDE) (Vol. 1, pp. 107–112).

[8] Nesterenko, M., Pogarsky, S., Katrich, V., & Pshenichnaya, S. (2024). Radiation Fields of Open Ring Microstrip Antenna. In 2024 IEEE 29th International Seminar/Workshop on Direct and Inverse Problems of Electromagnetic and Acoustic Wave Theory (DIPED) (Vol. 1, pp. 99–102).

[9] Nesterenko, M., Katrich, V., Dumin, O., & Arkusha, Y. (2024). Electrodynamic Characteristics of Biconical Dipole with Complex Distributed Surface Impedance and Asymmetric Excitation. In 2024 IEEE 29th International Seminar/Workshop on Direct and Inverse Problems of Electromagnetic and Acoustic Wave Theory (DIPED) (Vol. 1, pp. 201–204).

[10] Ramyea, R., Kasthuri, N., Preethi, S., Preetha, K., Prithvic, R., Sanjeeth Babu, M. (2024). Metamaterial Inspired Layered Patch Antenna for Navigational Applications. In 2024 15th International Conference on Computing Communication and Networking Technologies (ICCCNT) (pp. 1–6).

[11] Shokri, M., Ghobadi, C., & Nourinia, J. (2023). Dual-Band Circularly Polarized Asymmetric Dipole Array Antenna for GPS L1 and L2 Bands. AEU - International Journal of Electronics and Communications, 170, 154753.

[12] Balanis, C. A. (1997). Antenna Theory: Analysis & Design (2nd ed.). John Wiley & Sons, Inc.

[13] Sahana, C., Nirmala Devi, M., & Jayakumar, M. (2023). Hexagonal-Triangular Combinatorial Structure Based Dual-Band Circularly Polarized Patch Antenna for GAGAN Receivers. IEEE Access, 11, 23205–23216.

[14] Wang, H., Zhang, B., Liu, X., Yang, X., Zhang, R., & Wang, Y. (2024). Dual-band circular polarized microstrip antenna for GNSS application. Frequenz, 2024(ahead-of-print).

[15] James, J. R., & Hall, P. S. (1993). Handbook of Microstrip Antennas (IEEE electromagnetic, wave series, p. 28). Institution of Electrical Engineers.